HHS Public Access

Author manuscript

Immunity. Author manuscript; available in PMC 2019 October 01.

Published in final edited form as:

Immunity. 2016 April 19; 44(4): 782–794. doi:10.1016/j.immuni.2016.01.015.

Low voltage-activated $Ca_V3.1$ calcium channels in T cells: A role in shaping the immune response

Huiyun Wang[1], **Xuexin Zhang**[2], **Li Xue**[1], **Juan Xing**[3], **Marie-Hélène Jouvin**[1], **James W. Putney**[3], **Matthew P. Anderson**[4], **Mohamed Trebak**[2], **Jean-Pierre Kinet**[1,*]

[1]Department of Pathology, Beth Israel Deaconess Medical Center and Harvard Medical School, Boston, MA 02115, USA

[2]Department of Cellular and Molecular Physiology, Penn State University College of Medicine, Hershey, PA 17033, USA

[3]Laboratory of Signal Transduction, NIEHS, National Institutes of Health, Research Triangle Park, NC 27709, USA

[4]Departments of Neurology and Pathology, Beth Israel Deaconess Medical Center and Harvard Medical School, Boston, MA 02115, USA

SUMMARY

Activation of T cells is mediated by the engagement of T cell receptors (TCR) followed by calcium entry via store-operated calcium channels. Here we have shown an additional route for calcium entry into T cells – through the low voltage-activated T-type $Ca_V3.1$ calcium channel. $Ca_V3.1$ mediated a substantial current at resting membrane potentials, and its deficiency had no effect on TCR-initiated calcium entry. Mice deficient for $Ca_V3.1$ were resistant to the induction of experimental autoimmune encephalomyelitis, and had reduced productions of the granulocyte-macrophage colony-stimulating factor (GM-CSF) by central nervous system (CNS)-infiltrating T helper 1 (Th1) and Th17 cells. $Ca_V3.1$ deficiency led to decreased secretion of GM-CSF from *in vitro* polarized Th1 and Th17 cells. Nuclear translocation of the nuclear factor of activated T cell (NFAT) was also reduced in $Ca_V3.1$-deficient T cells. These data provide evidence for T-type channels in immune cells and their potential role in shaping the autoimmune response.

*Correspondence and requests for materials should be addressed to J.-P.K. (jkinet@bidmc.harvard.edu).

Author contributions H.W. designed and executed most experiments, generated the *Cacna1g*$^{flox/-}$*Lck-cre* animals and wrote the manuscript; X.Z. performed the electrophysiology experiments; L.X. performed some experiments and generated the *Cacna1g*$^{-/-}$ animals; J.X. performed the FLIPR experiments; M.-H.J.: designed the flow cytometry experiments and wrote the manuscript; J.W.P. designed the FLIPR experiments; M.P.A provided the *Cacna1g*$^{flox/flox}$ animals, and assisted in directing and designing the FLIPR experiments; M.T. designed the electrophysiology experiments; J.-P.K. designed the overall study. All authors commented on the manuscript.

Supplemental Information including four Figures and Supplemental Experimental Procedures can be found with this article online.

INTRODUCTION

Innumerable biological processes share calcium as a second messenger in virtually all types of cells, including immune cells. The bivalent cation calcium serves as a key mediator of T cell signaling. Calcineurin, a calcium-dependent serine-threonine phosphatase, activates T cells through the nuclear factor of activated T cell (NFAT) pathway. Cyclosporine A and tacrolimus, two calcineurin inhibitors, have been used for decades in the treatment of autoimmune diseases and the prevention of chronic allograft rejection (Schreiber and Crabtree, 1992).

We and others have demonstrated a clear role for a store-operated calcium (SOC) channel in mast cell activation (Hoth and Penner, 1992; Vig et al., 2008) and T cell activation (Oh-Hora et al., 2008). Lymphocytes are believed to use SOC entry (SOCE) as the main mode of calcium influx after T cell antigen receptor (TCR) engagement. The best characterized SOC channels in lymphocytes are known as ‘calcium release–activated calcium’ (CRAC) channels (Feske et al., 2001; Lewis and Cahalan, 1989; Parekh and Putney, 2005; Zweifach and Lewis, 1993), which leads to the calcium influx that drives TCR-initiated T cell activation (Feske et al., 2012).

Voltage-activated calcium channels (VOCCs) are expressed in excitable cells where they are activated by action potentials and are further subdivided into L-types ($Ca_V1.1$, $Ca_V1.2$, $Ca_V1.3$ and $Ca_V1.4$), P/Q-type ($Ca_V2.1$), N-type ($Ca_V2.2$), R-type (Cav2.3), and T-types (Cav3.1, Cav3.2 and Cav3.3) (Christel and Lee, 2012). These channels differ by their α1 chains, one of the 5 subunits of VOCCs (along with auxiliary α2, δ β *and* γ) and the one that forms the pore. These types of channels also differ in their tissue distribution and their role. In excitable cells, VOCCs serve as the major routes of calcium entry and regulate multiple functions such as muscle contraction, neurotransmitter release, synaptic plasticity, gene transcription, and neuropathic pain (Clapham, 2007; Gomez-Ospina et al., 2006; Zamponi et al., 2009).

In contrast to CRAC channels, VOCCs in lymphocytes have only been recently identified. Normal T cells express messages for β4 and α1 subunits of $Ca_V1.1$, 1.2, 1.3 and 1.4, and possibly $Ca_V2.1$ and $Ca_V2.2$ (Badou et al., 2013; Omilusik et al., 2013; Robert et al., 2011; Suzuki et al., 2010). In T cells from the β4 lethargic mice, NFAT translocation in response to interleukin-2 (IL-2) stimulation, and IL-4 and interferon-γ (IFN-γ) production after anti-CD3 and anti-CD28 stimulation are decreased (Badou et al., 2006).

Additionally, β3 deficient mice have a defective survival of naïve $CD8^+$ T lymphocytes (Jha et al., 2009). Mice with a conventional $Ca_V1.4$ deficiency display a decreased calcium influx, which is independent of SOCE, and a decreased Ras-extracellular signal-regulated kinase (ERK) and NFAT activation in response to TCR stimulation (Omilusik et al., 2011). However, whether $Ca_V1.4$ deficient mice exhibit an immune phenotype *in vivo* is unknown. $Ca_V1.2$ and $Ca_V1.3$ channels play a role in T helper 2 (Th2) cell activation, and their deficiency prevents the development of experimental asthma (Cabral et al., 2010; Robert et al., 2014).

The hallmarks of T-type calcium channels are low voltage-activated calcium current, fast (transient) inactivation kinetics, and low unitary conductance (Yunker and McEnery, 2003). T-type calcium channels are expressed in many developing tissues, e.g., skeletal and heart myocytes and neurons, and are important in regulating cellular phenotype transitions that lead to cell proliferation, differentiation, growth and death (Lory et al., 2006). $Ca_V3.1$, an α1 subunit encoded by *Cacna1g*, is known to be involved in sleep control, absence seizures in the thalamus, pacemaking in the sinoatrial node, and recovery of myocardial function after myocardial infarction (Huc et al., 2009). Accumulating evidence reveals that T-type channels are found throughout the body in a host of non-neural, noncardiovascular tissues, e.g., endocrine tissues, fibroblasts, bone, lung, spleen, liver, gastrointestinal tract, pancreas, kidney, ovary and testis (Yunker and McEnery, 2003).

To date, T-type calcium channels have not been reported to be expressed in lymphocytes or other immune cell subsets. The average membrane potential of lymphocytes has been measured to be between −60 and −55 mV (Rink et al., 1980). Among VOCCs, T-type calcium channels have the lowest activation thresholds at −70 mV (Perez-Reyes, 2003). Since these channels would be active in the range of resting membrane potentials of lymphocytes, we reasoned that T-type calcium channels, if present in lymphocytes and are functional with the voltage-dependence observed in other tissues, could play pivotal roles independently of TCR engagement. Here we used *in vitro* and *in vivo* techniques to investigate the presence of, and potential roles for, T-type calcium channels in T cells. We found that calcium entry through $Ca_V3.1$ is critical in GM-CSF, IL-17A, IL-17F, and IL-21 cytokine production in T cells.

RESULTS

$Ca_V3.1$ is expressed on the surface of $CD4^+$ T cells

We first investigated whether $Ca_V3.1$ is expressed in T cells. We performed quantitative RT-PCR in $CD4^+$ T cells from mouse lymph nodes, spleen, and thymus as well as splenic naïve and memory $CD4^+$ T cells. $Ca_V3.1$ was expressed in all of these T cell populations (Figure 1A) at the amounts lower than those observed in the cerebrum or in the cerebellum (Figure 1B). To assess $Ca_V3.1$ protein expression, we generated an antibody specific to $Ca_V3.1$ by immunizing with a peptide unique to $Ca_V3.1$ among VOCCs, and selecting for antibodies reactive to the same peptide. The specificity of this antibody was tested on human embryonic kidney cells (HEK 293) transfected with either a myc-tagged cDNA for Cav3.1, or the empty vector. This anti-Cav3.1 or an anti-myc antibody immunoprecipitated and immunoblotted a band of the expected size, about 250kD, from HEK 293 transfected with Cav3.1, but not from HEK 293 transfected with the empty vector (Figure S1A). This anti-$Ca_V3.1$ antibody was used to assay lysates of mouse $CD4^+$ T cells by immunoprecipitation and immunoblotting. $Ca_V3.1$ protein was detected in mouse $CD4^+$ T cell lysate following anti-$Ca_V3.1$ antibody immunoprecipitation, which was absent in control IgG immunoprecipitated proteins (Figure 1C). Therefore, $Ca_V3.1$ message and full-length $Ca_V3.1$ protein are indeed expressed in T cells.

To determine whether $Ca_V3.1$ is expressed at the plasma membrane of T cells, we performed surface biotinylation of mouse $CD4^+$ T cells followed by purification of biotinylated proteins

on an avidin column. In the eluate of the avidin column a band of the expected size for $Ca_V3.1$ was identified after blotting with anti-$Ca_V3.1$, while blotting with an antibody against the strictly intracellular protein,Gata-3, was negative (Figure 1D, lane B). In the flow-through, non-biotinylated fraction of the avidin column, both $Ca_V3.1$ and Gata-3 were detected (Figure 1D, lane N). These results established that $Ca_V3.1$ is present on the surface of $CD4^+$ T cells.

As tools for subsequent studies, we generated two strains of mice. Mice with a constitutive deletion of *Cacna1g* were generated by homologous recombination (Figure S2). These *Cacna1g*$^{-/-}$ mice were born with the expected frequency, did not display any gross abnormalities, developed normally, were of normal fertility, and could reach at least 17 months of age, all of which are similar to the findings reported for another strain of *Cacna1g*$^{-/-}$ mice (Kim et al., 2001). We also generated a mouse strain with a T cell-specific *Cacna1g* deficiency (*Cacna1g*$^{flox/-}$*Lck-cre*) through Cre-lox recombination, with Cre under the control of the T cell-specific Lck promoter. Using quantitative RT-PCR, we found a 60% reduction in $Ca_V3.1$ message in $CD4^+$ T cells from *Cacna1g*$^{flox/-}$*Lck-cre* animals, as compared to the near complete deficiency of message observed in cells from *Cacna1g*$^{-/-}$ animals (Figure 1E, upper panel). We also found compensatory increased expression of $Ca_V3.2$ and $Ca_V3.3$ in *Cacna1g*$^{-/-}$ and *Cacna1g*$^{flox/-}$*Lck-cre* $CD4^+$ T cells as compared to wild type (WT) $CD4^+$ T cells (Figure 1E, middle and lower panel).

Using the anti-$Ca_V3.1$ antibody that we developed, we confirmed that the $Ca_V3.1$ protein could not be detected in $CD4^+$ T cells, cerebrum and cerebellum from the *Cacna1g*$^{-/-}$ mice while it was detected in those from the WT mice (Figure 1F). We further demonstrated that the genetic deletion of $Ca_V3.1$ was complete in our *Cacna1g*$^{-/-}$ mice as there was no shorter splice variant presented in cerebellum (Figure S1B). At the same time, these data also verified the specificity of our anti-$Ca_V3.1$ antibody.

$Ca_V3.1$ in $CD4^+$ T cells carries a characteristic T-type current

We next assessed whether $Ca_V3.1$ in T cells acts as a functional channel, and, if so, whether it displays properties similar to those of $Ca_V3.1$ channels in other tissues. Whole-cell voltage-clamp recordings were conducted in primary splenic $CD4^+$ T cells from WT mice. Without exception, currents displayed a unique T-type channel profile (Nilius et al., 1985; Perez-Reyes, 2003) (Figure 2A–C and Figure S3A–D), with an activation threshold at −70 mV, a symmetric current-voltage (I-V) relationship, and rapid kinetics. The reported resting membrane potentials of WT lymphocyte are between −60 mV and −55 mV (Rink et al., 1980). These are within the range of T-type channel window currents as indicated by the Boltzmann fits of T-type channel activation and inactivation curves. The T-type channel currents were substantial at membrane potentials ranging from −65 mV to −25 mV (Figure S3E–H). The current densities at −60mv, −55mv and −50 mV were 0.29, 1.01 and 1.42 pA/pF, respectively (Figure S3F), similar to or exceeding those of CRAC channels (Parekh and Putney, 2005). In cells from *Cacna1g*$^{-/-}$ littermates, the current was markedly reduced (Figure 2A). Currents were 13.3 ± 1.38 pA in WT versus 6.95 ± 1.10 pA in *Cacna1g*$^{-/-}$ cells at −30 mV. The residual current in *Cacna1g*$^{-/-}$ cells retained the characteristics of T-type currents and was likely due to the observed compensatory expression of $Ca_V3.2$ and $Ca_V3.3$

channels (Figure 1E). Treatment with mibefradil, a channel blocker that preferentially targets T-type channels over L-type channels (Martin et al., 2000), essentially abrogated the currents in both WT and *Cacna1g*$^{-/-}$ cells (Figure 2A–B). In addition, upon treatment with the potent L-type calcium channel agonist, Bay K8644, the WT current was unaffected (Figure 2C). Taken together, these data demonstrate that multiple T-type calcium channel subtypes, including Cav3.1, are expressed and functional as calcium channels in T cells and mediate a substantial current with a low voltage activation threshold.

Single-channel recordings from CD4$^+$ T cells (Figure 2E–F) were characteristic of T-type channels, displaying a small single channel conductance of 7.5 pS, as reported for T-type channels cloned from the brain (Perez-Reyes et al., 1998). Based on these single-channel recordings, we estimate that a population of 200 to 400 T-type channels is expressed per T cell. The fast inactivation kinetics of the WT current, with a time constant of ~30 ms at −40 mV, closely matches that of $Ca_V3.1$ [Figure 2D; cf. inactivation time constants at −45 mV of cloned channels: $Ca_V3.1$ (30 ms), $Ca_V3.2$ (47 ms), $Ca_V3.3$ (137 ms) (Klockner et al., 1999)]. In *Cacna1g*$^{-/-}$ cells, the increase of this time constant to ~70 ms and the slight rightward shift in the I-V peak [peak currents for $Ca_V3.3$ channels occurred at slightly higher potentials (Klockner et al., 1999; Park et al., 2006)] were consistent with the observed compensatory upregulation of $Ca_V3.2$ and $Ca_V3.3$ expression in *Cacna1g*$^{-/-}$ cells. We therefore concluded that $Ca_V3.1$ is the functionally predominant subtype among the low-voltage-activated T-type calcium channels expressed in WT T cells.

$Ca_V3.1$-mediated calcium entry is independent of SOCE

We then investigated whether calcium influx via $Ca_V3.1$ channels may regulate or mediate signaling downstream of TCRs. We first used a standard method for activating CRAC channels, treatment with thapsigargin. Calcium influx triggered by thapsigargin was indistinguishable in CD4$^+$ T cells from WT and *Cacna1g*$^{-/-}$ littermates (Figure 3A). We next stimulated CD4$^+$ T cells with an anti-mouse CD3 antibody and again found no differences in calcium influx between WT and *Cacna1g*$^{-/-}$ cells (Figure 3B). We therefore observed no role for $Ca_V3.1$ in TCR-initiated signaling. Consistent with this finding, we observed no change in CRAC currents following treatment with mibefradil (Figure 3C–F). T-type currents were not detected in CRAC channel recording for several reasons: 1) reverse voltage ramps are designed to generally inhibit VOCCs; 2) the holding potential of 0 mV inactivates $Ca_V3.1$ channels; and 3) T-type channel recovery from slow and fast inactivation requires hundreds of ms to over 1 s (Perez-Reyes, 2003).

$Ca_V3.1$ does not play a role in T cell development and maturation

We then explored a potential role for $Ca_V3.1$ in T cell maturation. Analysis of CD4$^+$CD8$^-$ single positive (SP), CD4$^-$CD8$^+$ SP, CD4$^+$CD8$^+$ double positive (DP), CD4$^-$CD8$^-$ double negative 1 (DN1, CD44$^+$CD25$^-$), DN2 (CD44$^+$CD25$^+$), DN3 (CD44$^-$CD25$^+$) and DN4 (CD44$^-$CD25$^-$) cells indicated normal staging of the maturation of *Cacna1g*$^{-/-}$ thymocytes. No significant differences in the expression of TCRαβ in either DP or CD4$^+$CD8$^-$ SP cells, or in different maturation stages of CD4$^+$CD8$^-$ SP cells (CD69 and CD62L) were observed between WT and *Cacna1g*$^{-/-}$ thymocytes (Figure S4A–B). Nor were differences found in the expression of CD4, CD8 or TCRαβ in peripheral T lymphocytes (Figure S4C–D), or the

rates of proliferation in splenic $CD4^+$ T cells (Figure S4E–F). Taken together, these results demonstrate that $Ca_V3.1$ does not play a role in the development and maturation of $CD4^+$ or $CD8^+$ T cells.

$Ca_V3.1$ deficient mice are resistant to experimental autoimmune encephalomyelitis (EAE) induction

To further investigate the role of $Ca_V3.1$, we conducted *in vivo* studies using the EAE model. Animals were immunized with myelin oligodendrocyte glycoprotein peptide (MOG). WT animals developed paresis and displayed remitting and relapsing symptoms. In contrast, *Cacna1g*$^{-/-}$ mice were markedly resistant to EAE induction. In *Cacna1g*$^{-/-}$ mice, paresis was delayed or absent (Figure 4A upper panel, $P < 0.005$) and weight loss was reduced or did not occur (Figure 4A lower panel, $P < 0.005$). Histological analysis stained either by hematoxylin&eosin (H&E) or luxol fast blue (LFB) showed that the spinal cords of *Cacna1g*$^{-/-}$ mice were protected from inflammation and demyelination (Figure 4C). To assess whether the protection against EAE in *Cacna1g*$^{-/-}$ mice was due to the absence of $Ca_V3.1$ in T cells, we conducted additional EAE studies using our $Ca_V3.1$ ΔT mice with a T cell-specific $Ca_V3.1$ deficiency. Even with only partial (60%) reduction in $Ca_V3.1$ expression in *Cacna1g*$^{flox/-}$*Lck-cre* cells, paresis was delayed or absent (Figure 4B upper panel, $P < 0.0005$), weight loss was reduced or did not occur (Figure 4B lower panel, $P < 0.0005$), and no cases of complete paralysis occurred, while four of 16 WT mice had to be euthanized early due to complete paralysis. The spinal cords of the WT mice showed multiple foci of inflammation and demyelination, whereas such lesions were rare or absent in *Cacna1g*$^{flox/-}$*Lck-cre* mice (Figure 4D).

Since granulocyte-macrophage colony stimulating factor (GM-CSF) has proven to be a critical factor in the encephalitogenicity of both Th1 and Th17 cells in EAE model (Codarri et al., 2011; El-Behi et al., 2011), we analyzed the infiltrating cells in the central nervous system (CNS). We found that CNS from *Cacna1g*$^{flox/-}$*Lck-cre* mice had both reduced percentage and reduced absolute number of infiltrating $CD4^+$ T cells (Figure 4E–G). Notably, WT $CD4^+$ T cells produced GM-CSF, but the percentage of GM-CSF-producing $CD4^+$ T cells in *Cacna1g*$^{flox/-}$*Lck-cre* mice was reduced by 47% and the absolute number of these cells was reduced by 76%. CNS-infiltrating Th1 ($CD4^+$IFN-γ^+) and Th17 ($CD4^+$IL-$17A^+$) cells in *Cacna1g*$^{flox/-}$*Lck-cre* mice also produced less GM-CSF as compared to those in WT mice. Although *Cacna1g*$^{flox/-}$*Lck-cre* mice showed a reduction in both the percentage and absolute number of Th1 cells, only absolute number of Th17 cells was reduced in *Cacna1g*$^{flox/-}$*Lck-cre* mice. These results indicate that reduced production of GM-CSF by CNS-infiltrating Th1 and Th17 cells might be responsible to the EAE resistance in *Cacna1g*$^{flox/-}$*Lck-cre* mice.

$Ca_V3.1$ regulates Th cell signature cytokine production by *in vitro* polarized Th cells

We then investigated whether $Ca_V3.1$ played a role in Th cell signature cytokine production by *in vitro* polarized Th cells. We failed to observe any significant differences between *Cacna1g*$^{-/-}$ and WT mice in the percentage of $CD4^+$IFN-γ^+ Th1 cells, $CD4^+$TNF-α^+ Th1 cells, $CD4^+$IL-4^+ Th2 cells, or $CD4^+$Foxp3^+ regulatory T cells (Treg) following *in vitro* polarization of naïve $CD4^+$ cells in Th1, Th2, or Treg cell culture conditions (Figure 5A

upper panel and Figure 5B). However, using an *in vitro* Th17 cell culture condition, we observed a 32% reduction in $CD4^+IL\text{-}17A^+$ Th17 cells, 22% reduction in $CD4^+IL\text{-}17F^+$ Th17 cells, and 38% reduction in $CD4^+IL\text{-}21^+$ Th17 cells from *Cacna1g*$^{-/-}$ naïve $CD4^+$ cells compared to those from WT cells (Figure 5A lower panel and Figure 5B).

The transcriptional factors, T-bet and signal transducer as well as activator of transcription 3 (STAT3) and retinoid-related orphan receptor gamma t (RORγt) have been shown to be critical in Th1 and Th17 cell differentiation, respectively (Harris et al., 2007; Ivanov et al., 2006). We investigated whether these proteins decrease in *Cacna1g*$^{-/-}$ naïve $CD4^+$ cells following *in vitro* polarization. There was no difference in the amount of T-bet in either naïve $CD4^+$ cells or polarized Th1 cells from *Cacna1g*$^{-/-}$ and WT mice (Figure 5C left panel). The protein amounts of both phosphorylated STAT3 and RORγt were only detectable in polarized Th17 cells from both *Cacna1g*$^{-/-}$ and WT mice, and their amounts were lower in those from *Cacna1g*$^{-/-}$ compared to WT mice (Figure 5C middle and right panels).

$Ca_V3.1$ is up-regulated and mediates substantial calcium influx during *in vitro* Th17 polarization

To investigate the connection between $Ca_V3.1$ expression and *in vitro* Th cell polarization, we performed a time course experiment in WT naïve $CD4^+$ T cells. While there was no significant difference in $Ca_V3.1$ expression in cells within 12 hours of Th1 or Th2 cell polarization, it was noted that its expression was transiently elevated in cells from 3 hours to 12 hours of Th17 cell polarization (Figure 5D). Nevertheless, $Ca_V3.1$ expression diminished at 24 hours in all three culture conditions. To determine whether $Ca_V3.1$ expression correlates with calcium influx, we compared the intracellular free calcium ion concentration ($[Ca^{2+}]_i$) in resting splenic naive $CD4^+$ T cells and those following *in vitro* Th17 cell polarization for 12 hours from WT or *Cacna1g*$^{-/-}$ mice using Fura-2 AM single-cell calcium imaging. Constitutive calcium influxes in response to restoration of 2 mM extracellular calcium was significantly lower in both *Cacna1g*$^{-/-}$ naïve $CD4^+$ T cells (Figure 5E, left panel; peak $[Ca^{2+}]_i$, $P < 0.0001$; sustained $[Ca^{2+}]_i$ at 480s, $P < 0.0001$) and those following *in vitro* Th17 cell polarization (Figure 5E, right panel; peak $[Ca^{2+}]_i$, $P < 0.05$; sustained $[Ca^{2+}]_i$ at 480s, $P < 0.0001$) than those in wild-type cells. This suggests that $Ca_V3.1$ mediates constitutive calcium influx and raises $[Ca^{2+}]_i$ in WT T cells. Of note, a more sustained elevation of $[Ca^{2+}]_i$ in response to restoration of 2 mM extracellular calcium was observed in WT naïve $CD4^+$ T cells after 12 hours of Th17 cell polarization (Figure 5E; peak $[Ca^{2+}]_i$, $P < 0.05$; sustained $[Ca^{2+}]_i$ at 480s, $P < 0.0001$) compared to that in resting WT cells, indicating a correlation between $Ca_V3.1$ up-regulation and significant calcium influx during *in vitro* Th17 cell polarization.

$Ca_V3.1$ regulates GM-CSF production by *in vitro* polarized Th cells

We next investigate whether $Ca_V3.1$ regulates GM-CSF production by *in vitro* polarized Th1 and Th17 cells. We observed a 66% reduction in $CD4^+IFN\text{-}\gamma^+GM\text{-}CSF^+$ cells and a 45% reduction in $CD4^+IL\text{-}17A^+GM\text{-}CSF^+$ cells from *Cacna1g*$^{-/-}$ mice compared to those from WT mice following *in vitro* Th1 or Th17 cell polarization, respectively (Figure 6A–B).

NFAT proteins are calcium-dependent transcription factors and have been reported to be required for the production of GM-CSF (Johnson et al., 2004; Shang et al., 1999). NFATs primarily reside in a phosphorylated state in the cytoplasm of resting T cells. Once dephosphorylated by calmodulin-dependent phosphatase calcineurin, they translocate to the nucleus and activate target genes. To determine whether the function of $Ca_V3.1$ channel depends on NFAT activation, we assessed nuclear translocation of NFATc1 and NFATc2, two predominant species of NFAT in T cells (Johnson et al., 2004), in naïve $CD4^+$ T cells and those stimulated by anti-CD3 and anti-CD28 antibodies for 12 hours. We found both resting and stimulated cells from *Cacna1g*$^{-/-}$ mice had less nuclear NFATc1 and NFATc2 than those from WT mice (Figure 6C). Taken together, these data suggest that decreased nuclear translocation of NFAT might be related to the decreased GM-CSF production in *in vitro* polarized Th cells.

Cacna1g acute deletion confirms a similar *in vitro* phenotype

To address the issue of potential compensatory processes due to chronic absence of $Ca_V3.1$ during T cell development, we studied cytokine production in *in vitro* polarized Th cells with an acute deletion of *Cacna1g*. We infected naïve $CD4^+$ T cells harvested from *Cacna1g*$^{flox/flox}$ mice with a lentivirus encoding the CRE recombinase with GFP (+Cre) or with a control virus encoding GFP alone (control). After 72 hours of infection, the $CD4^+GFP^+$ cells were then sorted and subjected to Th1 or Th17 cell differentiation. Using quantitative RT-PCR, we found an 89% reduction in $Ca_V3.1$ message in $CD4^+GFP^+$ T cells with an acute *Cacna1g* deletion compared to cells infected by control vector (Figure 7A). We observed a 44% reduction in $CD4^+$IFN-γ^+GM-CSF^+ cells with an acute *Cacna1g* deletion compared to cells infected by control vector following *in vitro* Th1 cell polarization although there was, again, no difference between the $CD4^+$IFN-γ^+ cells from each group. We also observed 33%, 45%, 29% and 43% reduction in $CD4^+$IL-$17A^+$, $CD4^+$IL-$17A^+$GM-CSF^+, $CD4^+$IL-$17F^+$ and $CD4^+$IL-21^+ cells with an acute *Cacna1g* deletion compared to cells infected by control vector following *in vitro* Th17 cell polarization, respectively (Figure 7B–C). This shows that Cav3.1 deficiency during Th cell differentiation, and not during T cell development, is responsible for the *in vitro* phenotypes.

DISCUSSION

In this study, we demonstrated that the low voltage-activated T-type $Ca_V3.1$ calcium channels are expressed on the surfaces of $CD4^+$ T cells and $Ca_V3.1$ is the functionally predominant T-type calcium channel subtype in T cells. $Ca_V3.1$ functions as a VOCC and mediates a substantial current at resting membrane potentials. $Ca_V3.1$ deficiency decreases intracellular calcium concentration and has no effect on TCR-initiated calcium entry. We found that $Ca_V3.1$ deficiency inhibits the autoimmune response in the EAE model as well as reduces GM-CSF production from CNS-infiltrating Th1 and Th17 cells. The *in vitro* polarized Th17 cells from *Cacna1g*$^{-/-}$ naïve $CD4^+$ T cells showed decreased IL-17A, IL-17F, and IL-21 production. In consistence with *in vivo* studies, GM-CSF production from both *in vitro* polarized *Cacna1g*$^{-/-}$ Th1 and Th17 cells was reduced. Subsequent studies have shown that $Ca_V3.1$ deficiency results in decreased nuclear translocation of NFAT proteins.

In $CD4^+$ T cells, we found that the current mediated by T-type channels is of unanticipated magnitude, comparable to or greater than that of CRAC channels, and T-type channels operate independently of TCR engagement and are not involved in store operated calcium entry. T-type channels, unlike CRAC channels and relative to other VOCCs, have a lower voltage threshold for activation and can generate large calcium transients in the range of resting negative membrane potentials of T cells, at which the driving force for calcium entry is large. Ca_V3 channel subunits have the same molecular organization as Ca_V1 and Ca_V2 channels but are only ~25% identical in amino acid sequence. One of the unique features of Ca_V3 channels, unlike Ca_V1 and Ca_V2 channels, is that their α1 subunits function independently of other subunits (Catterall, 2011). These could in part explain the differences in immune phenotypes between $Ca_V3.1$ deficient mice and mice with abnormalities of L-type channels or the β subunits.

Our understanding of the mechanisms in T cells that underlie the pathogenesis of multiple sclerosis is constantly evolving. Th1 cells were initially thought to be responsible for EAE, and most recently, Th17 cells. However, neither signature cytokines for Th1 (IFN-γ) nor for Th17 (IL-17A, IL-17F, and IL-21) cells are required for the development of EAE (Chu et al., 2000; Coquet et al., 2008; Haak et al., 2009). Instead, GM-CSF, produced by both Th1 and Th17 cells (Codarri et al., 2011; El-Behi et al., 2011; Lin et al., 2014; McQualter et al., 2001), is the only known cytokine produced by T cells that is required for susceptibility to EAE.

GM-CSF is a hematopoietic growth factor originally identified as a stimulator for the proliferation of granulocytes and macrophages from bone marrow precursor cells. GM-CSF is produced by a large variety of cells including activated T and B cells, monocytes, macrophages, endothelial cells, fibroblasts and other sources. Production of GM-CSF in T cells, stimulated by IL-1β and IL-23 in mice, is essential for encephalitogenicity in EAE (Codarri et al., 2011; El-Behi et al., 2011). GM-CSF induces the proliferation and activation of microglial cells including neurotoxic M1-like phenotype of microglia, which is required for the onset of EAE (Ponomarev et al., 2007). Furthermore, GM-CSF-producing $CD4^+$ T cells upregulate the production of proinflammatory mediators such as IL-1β, IL-6, and TNF-α, which contribute to myelin sheath damage via upregulation of toll-like receptor (TLR) and CD14 expression (Parajuli et al., 2012).

Collective evidence has shown that calcium signaling is critical in the regulation of GM-CSF gene expression. Activation of GM-CSF expression by calcium occurs through the phosphatase calcineurin (Shannon et al., 1997) and its expression is inhibited by immunosuppressive agents such as cyclosporine A (Hatfield and Roehm, 1992; Tsuboi et al., 1994). In lymphocytes, NFAT is reported to be required for the production of GMCSF by the formation of DNase I hypersensitive sites within enhancers (Johnson et al., 2004; Shang et al., 1999). Its NFAT dependence is further evidenced by the reduction of inducible GM-CSF expression by either a selective NFAT-inhibitory peptide (Aramburu et al., 1999) or genetic deletion of both NFATc1 and NFATc2 proteins (Peng et al., 2001).

T cell activation induces an increase in intracellular calcium concentrations and the activation of the phosphatase calcineurin, which in turn dephosphorylates NFAT proteins.

Because of the presence of constitutively active intracellular kinases that rephosphorylate and inactivate NFAT, calcineurin is continuously needed to maintain NFAT proteins in an active state. As a result, NFAT is optimally activated in conditions of low sustained increases of intracellular calcium (MaciaÂn et al., 2001). The decreased intracellular calcium concentration and nuclear translocation of NFAT in *Cacna1g*$^{-/-}$ cells indicate that $Ca_V3.1$ channel may play a critical role in maintaining a sustained increase of intracellular calcium and activity of NFAT, and thus in inducing transcriptional activation of GM-CSF. NFATc1, NFATc2 or NFATc1/NFATc2 double deficient mice are protected from EAE and CNS infiltrating GM-CSF-producing $CD4^+$ T cells are diminished in these mice (Dietz et al., 2015; Reppert et al., 2015).

NFAT proteins have been reported to be necessary for the gene expressions of many cytokines and transcription factors critical for T cell differentiation, including IL-2 for naïve T cells, IFN-γ and T-bet for Th1 cells, IL-4 and GATA3 for Th2 cells, Foxp3 for Treg cells as well as IL-17, IL-21 and RORγt for Th17 cells (Hermann-Kleiter and Baier, 2010). It is unclear why altered NFAT activity by $Ca_V3.1$ deficiency only selectively affects GM-CSF and Th17 cell signature cytokine production both *in vivo* and *in vitro* as well as Th1 signature cytokine production *in vivo*. The exquisite balance between activities of NFATc1 and NFATc2 induced by $Ca_V3.1$ calcium channel might be the key for the distinct biological outcomes.

In conclusion, our results show that T-type calcium channels are expressed and functional in T cells in a TCR-independent manner. These $Ca_V3.1$ channels may play a key role in regulating GM-CSF secretion from T cells, and targeted deficiency of these channels results in a reduced autoimmune response in EAE. Given the mild phenotype of conventionally deficient mice, a global targeting of $Ca_V3.1$ appears to be a possible new therapeutic approach for multiple sclerosis. Future studies can further elucidate the roles and elements of signaling pathways in T cells regulated by $Ca_V3.1$ and by other T-type calcium channels.

EXPERIMENTAL PROCEDURES

Generation of *Cacna1g*$^{-/-}$ animals

A targeting construct was designed to genetically delete the pore region of $Ca_V3.1$ by using a neomycin cassette to replace the exons 11 to 13. The targeting construct was transfected into 129/SvJ embryonic stem (ES) cells. Targeted ES clones were identified by Southern blotting and used in the generation of germline chimeras. Heterozygous germline mice (129/SvJ) were interbred to obtain homozygous mice. Male germline chimeras were also backcrossed with female C57BL/6 mice. Homologous recombination was verified by Southern blotting, PCR and immunoblotting. WT and *Cacna1g*$^{-/-}$ littermates (6–12 weeks) were used for phenotypic analysis. Animals were maintained at the full barrier facility of the Center of Life Sciences which is fully accredited by AAALAC and the U.S. Department of Agriculture.

Generation of *Cacna1g*$^{flox/-}$*Lck-cre* animals

To generate animals with a T cell-specific $Ca_V3.1$ deficiency, constitutive *Cacna1g*$^{-/-}$ mice were crossed with a transgenic strain expressing Cre under the control of the Lck promoter [B6.Cg-Tg(Lck-cre)1Cwi N9 mice from Taconic]. The resulting pups that were *Cacna1g*$^{+/-}$ and transgenic for lck-Cre were crossed with a strain with two floxed 1G alleles provided by Matthew Anderson (Anderson et al., 2005). The resulting pups that were *Cacna1g*$^{flox/-}$ and transgenic for lck-Cre have a $Ca_V3.1$ deficiency limited to T cells. Their *Cacna1g*$^{flox/+}$ littermates which were negative for Cre were used as control.

Electrophysiology

Electrophysiological recordings were carried out using an Axopatch 200B and Digidata 1440A (Axon Instruments) at room temperature. Only cells with tight seals (>16 GΩ) were selected to perform recording. Cells were maintained at a −90 mV holding potential during experiments. For whole-cell recording: voltage steps (10 mV increments from a holding potential of −90 mV up to +50 mV) lasting 250 ms were applied every 2 s. Bath solution: 120 mM tetraethylammonium chloride, 10 mM CsCl, 10 mM $CaCl_2$, 10 mM HEPES (pH 7.4). Pipette solution: 105 mM Cs-methanesulfonate, 10 mM Cs-1,2-*bis*-(2-aminophenoxy)ethane-*N*,*N*,*N*′,*N*′-tetraacetic acid (Cs-BAPTA), 5 mM $CaCl_2$, 8 mM $MgCl_2$, and 10 mM HEPES (pH 7.2). Calculated buffered intracellular calcium concentration is 150 nM using Maxchel software available online at http://maxchelator.stanford.edu. For cell-attached single-channel recording: cells were maintained at a holding potential of −90mV and voltage steps (10 mV increments from 30 mV up to 0 mV) lasting 250 ms were applied every 2 s. Bath solution: 145 mM KCl, 1 mM $CaCl_2$, 10 mM HEPES (pH 7.4). Pipette solution: 110 mM $CaCl_2$ or $BaCl_2$, 5 mM HEPES (pH 7.4). Clampfit 10.1 software was used for data analysis. Pipettes were pulled by a P-97 micropipette puller (Sutter Instrument Company) and polished with DMF1000 (World Precision Instruments).

EAE model

WT, *Cacna1g*$^{-/-}$ and *Cacna1g*$^{flox/-}$*Lck-cre* female littermates aged 10–12 weeks were used. At day 0 they were injected with myelin oligodendrocyte glycoprotein (MOG) and FA emulsion (Hooke Laboratories) containing 1 mg/ml MOG35–55 and 2 mg/ml killed mycobacterium tuberculosis H37R, into two sites in the upper and lower back (100 μL per site) subcutaneously. Within 2 hours the mice were intraperitoneally injected with pertussis toxin (165 ng in 100 ml PBS). The toxin injection was repeated 24 hours later. Mice were weighed and scored daily using the standard score as shown in bellow. Mice were observed up to day 30. For histology experiments, spinal cords were dissected from EAE mice, fixed in formalin, embedded in paraffin, sectioned and stained with hematoxylin and eosin (H&E) or Luxol fast blue (LFB).

Statistical analysis

For *Cacna1g* acute deletion flow cytometry experiments, paired Student *t* test with a two tailed distribution was used. For Fura-2 calcium imaging study, unpaired Student *t* test with

a two-tailed distribution was used. For the rest of the statistical analyses, we used Mann-Whitney *U* test.

Supplementary Material

Refer to Web version on PubMed Central for supplementary material.

Acknowledgements

This work was funded in part by NIH grants 5T32HL789315 to H.W., HL097111 to M.T., 5R01NS081916 to M.P.A., and 5R37GM53950 and 1R01AI095308 to J.-P.K. The authors have no conflicts of interest to disclose.

REFERENCES

Anderson MP, Mochizuki T, Xie J, Fischler W, Manger JP, Talley EM, Scammell TE, and Tonegawa S (2005). Thalamic Cav3.1 T-type Ca2+ channel plays a crucial role in stabilizing sleep. Proc Natl Acad Sci U S A 102, 1743–1748. [PubMed: 15677322]

Aramburu J, Yaffe MB, López-Rodríguez C, Cantley LC, Hogan PG, and Rao A (1999). Affinity-driven peptide selection of an NFAT inhibitor more selective than cyclosporin A. Science 285, 2129–2133. [PubMed: 10497131]

Badou A, Jha MK, Matza D, and Flavell RA (2013). Emerging roles of L-type voltage-gated and other calcium channels in T lymphocytes. Front Immunol 4.

Badou A, Jha MK, Matza D, Mehal WZ, Freichel M, Flockerzi V, and Flavell RA (2006). Critical role for the beta regulatory subunits of Cav channels in T lymphocyte function. Proc Natl Acad Sci U S A 103, 15529–15534. [PubMed: 17028169]

Cabral MD, Paulet PE, Robert V, Gomes B, Renoud ML, Savignac M, Leclerc C, Moreau M, Lair D, Langelot M, et al. (2010). Knocking down Cav1 calcium channels implicated in Th2 cell activation prevents experimental asthma. Am J Respir Crit Care Med 181, 1310–1317. [PubMed: 20167851]

Catterall WA (2011). Voltage-gated calcium channels. Cold Spring Harb Perspect Biol 3.

Christel C, and Lee A (2012). Ca2+-dependent modulation of voltage-gated Ca2+ channels. Biochim Biophys Acta 8, 24.

Chu C-Q, Wittmer S, and Dalton DK (2000). Failure to suppress the expansion of the activated CD4 T cell population in interferon γ–deficient mice leads to exacerbation of experimental autoimmune encephalomyelitis. The Journal of experimental medicine 192, 123–128. [PubMed: 10880533]

Clapham DE (2007). Calcium signaling. Cell 131, 1047–1058. [PubMed: 18083096]

Codarri L, Gyülvészi G, Tosevski V, Hesske L, Fontana A, Magnenat L, Suter T, and Becher B (2011). ROR [gamma] t drives production of the cytokine GM-CSF in helper T cells, which is essential for the effector phase of autoimmune neuroinflammation. Nature immunology 12, 560–567. [PubMed: 21516112]

Coquet JM, Chakravarti S, Smyth MJ, and Godfrey DI (2008). Cutting edge: IL-21 is not essential for Th17 differentiation or experimental autoimmune encephalomyelitis. The Journal of Immunology 180, 7097–7101. [PubMed: 18490706]

Dietz L, Frommer F, Vogel AL, Vaeth M, Serfling E, Waisman A, Buttmann M, and Berberich-Siebelt F (2015). NFAT1 deficit and NFAT2 deficit attenuate EAE via different mechanisms. European journal of immunology 45, 1377–1389. [PubMed: 25630465]

El-Behi M, Ciric B, Dai H, Yan Y, Cullimore M, Safavi F, Zhang G-X, Dittel BN, and Rostami A (2011). The encephalitogenicity of TH17 cells is dependent on IL-1-and IL-23-induced production of the cytokine GM-CSF. Nature immunology 12, 568–575. [PubMed: 21516111]

Feske S, Giltnane J, Dolmetsch R, Staudt LM, and Rao A (2001). Gene regulation mediated by calcium signals in T lymphocytes. Nat Immunol 2, 316–324. [PubMed: 11276202]

Feske S, Skolnik EY, and Prakriya M (2012). Ion channels and transporters in lymphocyte function and immunity. Nat Rev Immunol 12, 532–547. [PubMed: 22699833]

Gomez-Ospina N, Tsuruta F, Barreto-Chang O, Hu L, and Dolmetsch R (2006). The C terminus of the L-type voltage-gated calcium channel Ca V 1.2 encodes a transcription factor. Cell 127, 591–606. [PubMed: 17081980]

Haak S, Croxford AL, Kreymborg K, Heppner FL, Pouly S, Becher B, and Waisman A (2009). IL-17A and IL-17F do not contribute vitally to autoimmune neuro-inflammation in mice. The Journal of clinical investigation 119, 61. [PubMed: 19075395]

Harris TJ, Grosso JF, Yen H-R, Xin H, Kortylewski M, Albesiano E, Hipkiss EL, Getnet D, Goldberg MV, and Maris CH (2007). Cutting edge: An in vivo requirement for STAT3 signaling in TH17 development and TH17-dependent autoimmunity. The Journal of Immunology 179, 4313–4317. [PubMed: 17878325]

Hatfield SM, and Roehm NW (1992). Cyclosporine and FK506 inhibition of murine mast cell cytokine production. Journal of Pharmacology and Experimental Therapeutics 260, 680–688. [PubMed: 1371158]

Hermann-Kleiter N, and Baier G (2010). NFAT pulls the strings during CD4+ T helper cell effector functions. Blood 115, 2989–2997. [PubMed: 20103781]

Hoth M, and Penner R (1992). Depletion of intracellular calcium stores activates a calcium current in mast cells. Nature 355, 353–356. [PubMed: 1309940]

Huc S, Monteil A, Bidaud I, Barbara G, Chemin J, and Lory P (2009). Regulation of T-type calcium channels: signalling pathways and functional implications. Biochimica et Biophysica Acta (BBA)-Molecular Cell Research 1793, 947–952. [PubMed: 19071165]

Ivanov II, McKenzie BS, Zhou L, Tadokoro CE, Lepelley A, Lafaille JJ, Cua DJ, and Littman DR (2006). The orphan nuclear receptor RORγt directs the differentiation program of proinflammatory IL-17+ T helper cells. Cell 126, 1121–1133. [PubMed: 16990136]

Jha MK, Badou A, Meissner M, McRory JE, Freichel M, Flockerzi V, and Flavell RA (2009). Defective survival of naive CD8+ T lymphocytes in the absence of the β3 regulatory subunit of voltage-gated calcium channels. Nature immunology 10, 1275–1282. [PubMed: 19838200]

Johnson BV, Bert AG, Ryan GR, Condina A, and Cockerill PN (2004). Granulocyte-macrophage colony-stimulating factor enhancer activation requires cooperation between NFAT and AP-1 elements and is associated with extensive nucleosome reorganization. Molecular and cellular biology 24, 7914–7930. [PubMed: 15340054]

Kim D, Song I, Keum S, Lee T, Jeong M-J, Kim S-S, McEnery MW, and Shin H-S (2001). Lack of the burst firing of thalamocortical relay neurons and resistance to absence seizures in mice lacking Œ ± 1G T-type Ca 2+ channels. Neuron 31, 35–45. [PubMed: 11498049]

Klockner U, Lee JH, Cribbs LL, Daud A, Hescheler J, Pereverzev A, Perez-Reyes E, and Schneider T (1999). Comparison of the Ca2 + currents induced by expression of three cloned alpha1 subunits, alpha1G, alpha1H and alpha1I, of low-voltage-activated T-type Ca2 + channels. Eur J Neurosci 11, 4171–4178. [PubMed: 10594642]

Lewis RS, and Cahalan MD (1989). Mitogen-induced oscillations of cytosolic Ca2+ and transmembrane Ca2+ current in human leukemic T cells. Cell Regul 1, 99–112. [PubMed: 2519622]

Lin C-C, Bradstreet TR, Schwarzkopf EA, Sim J, Carrero JA, Chou C, Cook LE, Egawa T, Taneja R, and Murphy TL (2014). Bhlhe40 controls cytokine production by T cells and is essential for pathogenicity in autoimmune neuroinflammation. Nature communications 5.

Lory P, Bidaud I, and Chemin J (2006). T-type calcium channels in differentiation and proliferation. Cell Calcium 40, 135–146. [PubMed: 16797068]

MaciaÂn F, Lâopez-Rodrâiguez C, and Rao A (2001). Partners in transcription: NFAT and AP-1. Oncogene 20, 2476–2489. [PubMed: 11402342]

Martin RL, Lee J-H, Cribbs LL, Perez-Reyes E, and Hanck DA (2000). Mibefradil block of cloned T-type calcium channels. Journal of Pharmacology and Experimental Therapeutics 295, 302–308. [PubMed: 10991994]

McQualter JL, Darwiche R, Ewing C, Onuki M, Kay TW, Hamilton JA, Reid HH, and Bernard CC (2001). Granulocyte Macrophage Colony-Stimulating Factor A New Putative Therapeutic Target in Multiple Sclerosis. The Journal of experimental medicine 194, 873–882. [PubMed: 11581310]

Nilius B, Hess P, Lansman J, and Tsien R (1985). A novel type of cardiac calcium channel in ventricular cells.

Oh-Hora M, Yamashita M, Hogan PG, Sharma S, Lamperti E, Chung W, Prakriya M, Feske S, and Rao A (2008). Dual functions for the endoplasmic reticulum calcium sensors STIM1 and STIM2 in T cell activation and tolerance. Nat Immunol 9, 432–443. [PubMed: 18327260]

Omilusik K, Priatel JJ, Chen X, Wang YT, Xu H, Choi KB, Gopaul R, McIntyre-Smith A, Teh HS, Tan R, et al. (2011). The Ca(v)1.4 calcium channel is a critical regulator of T cell receptor signaling and naive T cell homeostasis. Immunity 35, 349–360. [PubMed: 21835646]

Omilusik KD, Nohara LL, Stanwood S, and Jefferies WA (2013). Weft, warp, and weave: the intricate tapestry of calcium channels regulating T lymphocyte function. Front Immunol 4.

Parajuli B, Sonobe Y, Kawanokuchi J, Doi Y, Noda M, Takeuchi H, Mizuno T, and Suzumura A (2012). GM-CSF increases LPS-induced production of proinflammatory mediators via upregulation of TLR4 and CD14 in murine microglia. J. Neuroinflammation 9.

Parekh AB, and Putney JW Jr. (2005). Store-operated calcium channels. Physiol Rev 85, 757–810. [PubMed: 15788710]

Park JY, Kang HW, Moon HJ, Huh SU, Jeong SW, Soldatov NM, and Lee JH (2006). Activation of protein kinase C augments T-type Ca2+ channel activity without changing channel surface density. J Physiol 577, 513–523. [PubMed: 17008378]

Peng SL, Gerth AJ, Ranger AM, and Glimcher LH (2001). NFATc1 and NFATc2 together control both T and B cell activation and differentiation. Immunity 14, 13–20. [PubMed: 11163226]

Perez-Reyes E (2003). Molecular physiology of low-voltage-activated t-type calcium channels. Physiol Rev 83, 117–161. [PubMed: 12506128]

Perez-Reyes E, Cribbs LL, Daud A, Lacerda AE, Barclay J, Williamson MP, Fox M, Rees M, and Lee J-H (1998). Molecular characterization of a neuronal low-voltage-activated T-type calcium channel. Nature 391, 896–900. [PubMed: 9495342]

Ponomarev ED, Shriver LP, Maresz K, Pedras-Vasconcelos J, Verthelyi D, and Dittel BN (2007). GM-CSF production by autoreactive T cells is required for the activation of microglial cells and the onset of experimental autoimmune encephalomyelitis. The Journal of Immunology 178, 39–48. [PubMed: 17182538]

Reppert S, Zinser E, Holzinger C, Sandrock L, Koch S, and Finotto S (2015). NFATc1 deficiency in T cells protects mice from experimental autoimmune encephalomyelitis. European journal of immunology.

Rink TJ, Montecucco C, Hesketh TR, and Tsien RY (1980). Lymphocyte membrane potential assessed with fluorescent probes. Biochim Biophys Acta 595, 15–30. [PubMed: 6153065]

Robert V, Triffaux E, Paulet PE, Guery JC, Pelletier L, and Savignac M (2014). Protein kinase C-dependent activation of CaV1.2 channels selectively controls human TH2-lymphocyte functions. J Allergy Clin Immunol 133, 1175–1183. [PubMed: 24365142]

Robert V, Triffaux E, Savignac M, and Pelletier L (2011). Calcium signalling in T-lymphocytes. Biochimie 93, 2087–2094. [PubMed: 21712067]

Schreiber SL, and Crabtree GR (1992). The mechanism of action of cyclosporin A and FK506. Immunol Today 13, 136–142. [PubMed: 1374612]

Shang C, Attema J, Cakouros D, Cockerill PN, and Shannon MF (1999). Nuclear factor of activated T cells contributes to the function of the CD28 response region of the granulocyte macrophage-colony stimulating factor promoter. International immunology 11, 1945–1956. [PubMed: 10590260]

Shannon MF, Coles LS, Vadas MA, and Cockerill PN (1997). Signals for activation of the GM-CSF promoter and enhancer in T cells. Critical Reviews™ in Immunology 17.

Suzuki Y, Inoue T, and Ra C (2010). L-type Ca 2+ channels: a new player in the regulation of Ca 2+ signaling, cell activation and cell survival in immune cells. Molecular immunology 47, 640–648. [PubMed: 19926136]

Tsuboi A, Masuda E, Naito Y, Tokumitsu H, Arai K, and Arai N (1994). Calcineurin potentiates activation of the granulocyte-macrophage colony-stimulating factor gene in T cells: involvement of the conserved lymphokine element 0. Molecular biology of the cell 5, 119–128. [PubMed: 8186461]

Vig M, DeHaven WI, Bird GS, Billingsley JM, Wang H, Rao PE, Hutchings AB, Jouvin MH, Putney JW, and Kinet JP (2008). Defective mast cell effector functions in mice lacking the CRACM1 pore subunit of store-operated calcium release-activated calcium channels. Nat Immunol 9, 89–96. [PubMed: 18059270]

Yunker AMR, and McEnery MW (2003). Low-voltage-activated ("T-Type") calcium channels in review. Journal of bioenergetics and biomembranes 35, 533–575. [PubMed: 15000520]

Zamponi GW, Lewis RJ, Todorovic SM, Arneric SP, and Snutch TP (2009). Role of voltage-gated calcium channels in ascending pain pathways. Brain Res Rev 60, 84–89. [PubMed: 19162069]

Zweifach A, and Lewis RS (1993). Mitogen-regulated Ca2+ current of T lymphocytes is activated by depletion of intracellular Ca2+ stores. Proc Natl Acad Sci U S A 90, 6295–6299. [PubMed: 8392195]

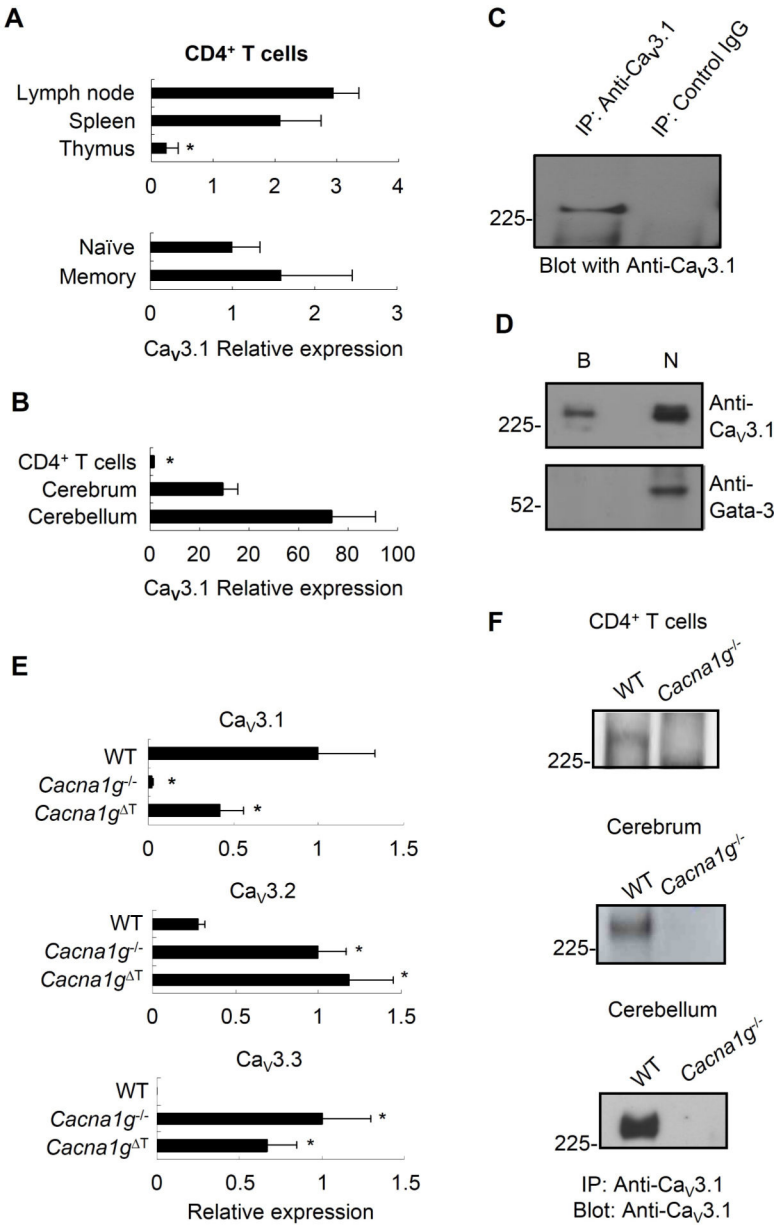

Figure 1. $Ca_V3.1$ is expressed in T cells and localized to the plasma membrane.

(A) Comparison of $Ca_V3.1$ expression by quantitative RT-PCR in $CD4^+$ T cells isolated from mouse lymph nodes, spleen and thymus (upper panel) as well as in splenic naïve and memory $CD4^+$ T cells (lower panel).

(B) Comparison of $Ca_V3.1$ expression by quantitative RT-PCR in mouse splenic $CD4^+$ T cells and cells isolated from cerebrum and cerebellum.

(C) $Ca_V3.1$ protein expression in pooled splenic and lymph node $CD4^+$ T cells after immunoprecipitating with anti-$Ca_V3.1$ antibody (anti-$Ca_V3.1$) or control rabbit IgG (control IgG), and then immunoblotting with anti-$Ca_V3.1$.

(D) The surface proteins fraction (lane B) and non-surface protein fraction (lane N) from mouse $CD4^+$ T cells immunoblotted by anti-$Ca_V3.1$ Ab (upper panel) or anti-GATA-3 Ab as control (lower panel).

(E) Relative expression of the $Ca_V3.1$, $Ca_V3.2$, and $Ca_V3.3$ message in $CD4^+$ T cells from WT, *Cacna1g*$^{-/-}$ and *Cacna1g*$^{flox/-}$*Lck-cre* mice.
(F) $Ca_V3.1$ protein expression in $CD4^+$ T cells, cerebrum and cerebellum from WT and *Cacna1g*$^{-/-}$ mice using anti-$Ca_V3.1$ antibody to immunoprecipitate and immunoblot. * $p < 0.05$ (Mann-Whitney *U* test). Data are from one experiment representative of three independent experiments with similar results (A-F; mean and s.e.m. in A,B,E).
Cacna1g$^{\Delta T}$ refers to *Cacna1g*$^{flox/-}$*Lck-cre*. See also Figure S1 and S2.

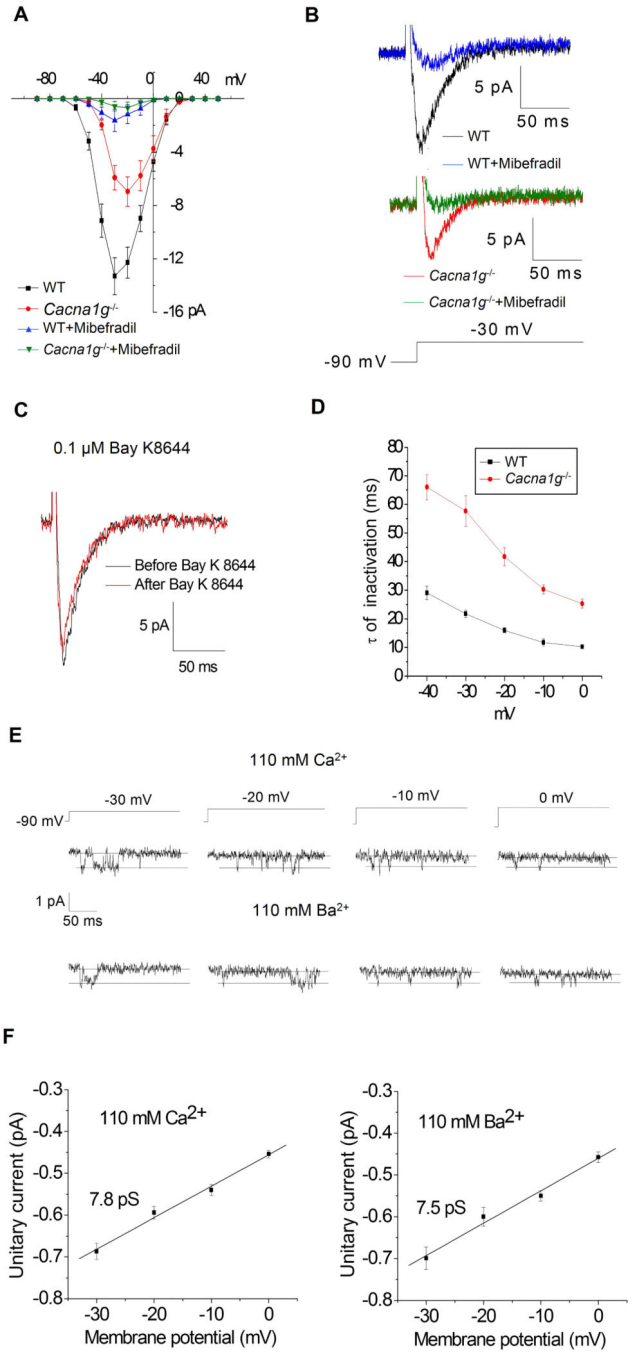

Figure 2. The signature current for T-type channels is present in WT CD4$^+$ T cells and reduced in *Cacna1g*$^{-/-}$ CD4$^+$ T cells.

(A) WT CD4$^+$ cells (n= 17) and *Cacna1g*$^{-/-}$ CD4$^+$ T cells (n=19) were subjected to whole-cell patch clamp recordings. Average I-V relationships are displayed. Recordings in both cell types were made in the absence or presence of the T-type channel inhibitor, mibefradil (1 μM). The bath solution contained 10 mM Ca^{2+}.

(B) Representative recordings at the −30 mV voltage step are displayed for all conditions.

(C) Representative recordings at −30 mV in WT CD4$^+$ T cells in the presence of Bay K8644 (0.1 μM).

(D) Time constant (τ) of voltage-dependent inactivation of currents in $CD4^+$ T cells elicited by voltage steps from a holding potential of −90 mV. Data represent means ± SEM from 7 WT and 8 *Cacna1g*$^{-/-}$ cells.

(E) Single-channel recordings: representative current records from WT $CD4^+$ T cells are shown below the associated voltage protocols.

(F) Unitary current-voltage relationships generated from 25 recordings with Ca^{2+} (left panel) or Ba^{2+} (right panel) as carrier. Straight lines are linear fits to the data, with slopes of 7.8 pS and 7.5 pS for Ca^{2+} and Ba^{2+}, respectively.

Data are from one experiment representative of at least three independent experiments with similar results (A-F; mean and s.e.m. in A,D,F). See also Figure S3.

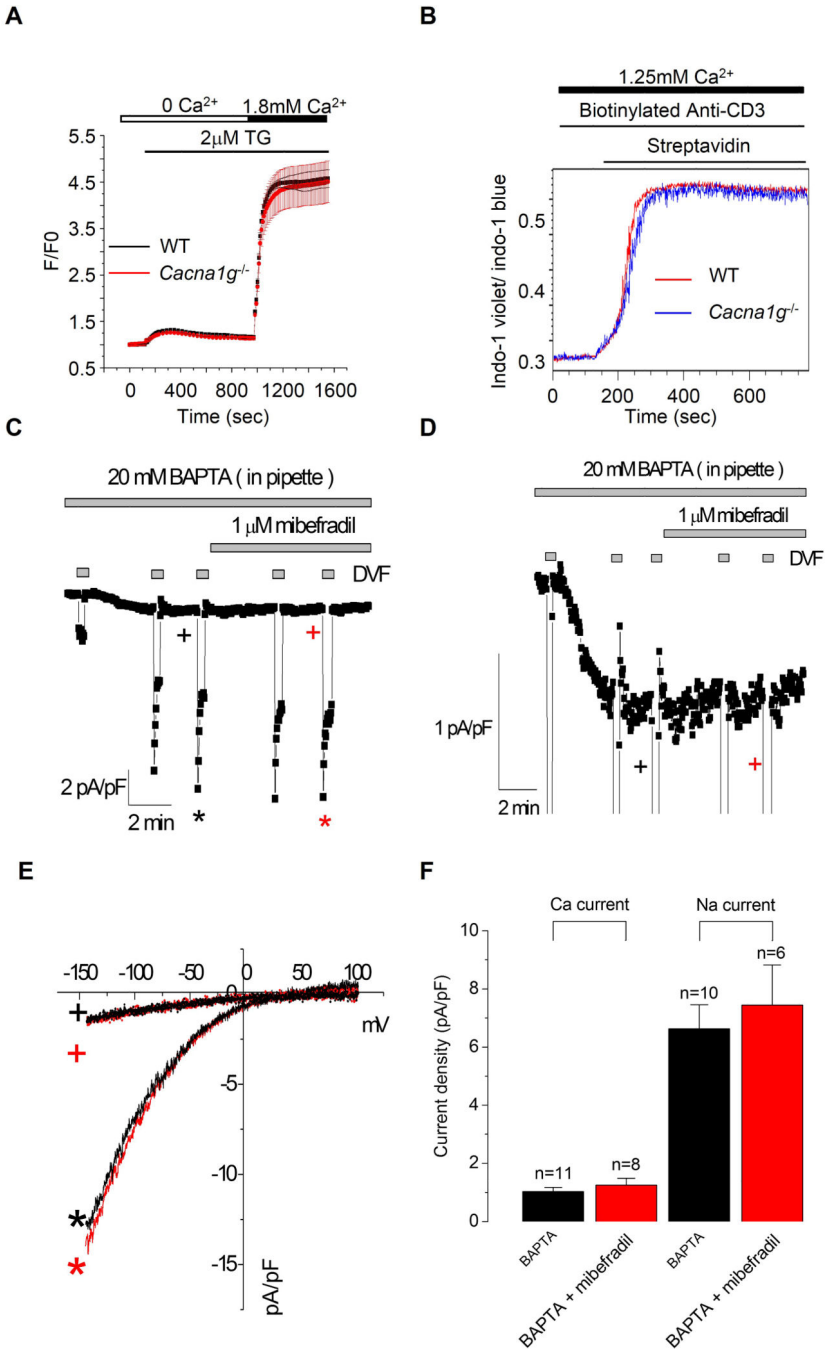

Figure 3. $Ca_V3.1$-mediated calcium entry is functionally independent of TCR engagement and SOCE.

(A) The effect of $Ca_V3.1$ deficiency in $CD4^+$ cells on Store-operated calcium entry triggered by thapsigargin (TG; 2 μM).

(B) Calcium entry in splenic $CD4^+$ cells from WT or *Cacna1g*$^{-/-}$ mice induced by TCR engagement measured using flow cytometry.

(C) Representative time course of whole-cell current at −100 mV with 0 mV holding potential from $CD4^+$ T cell in the presence of mibefradil (1 μM) and divalent-free (DVF) bath solution.

(D) An enlarged view of C.
(E-F) Current-voltage (I-V) relationships (E) and statistics (F).
Data are from one experiment representative of three independent experiments with similar results (A-F).

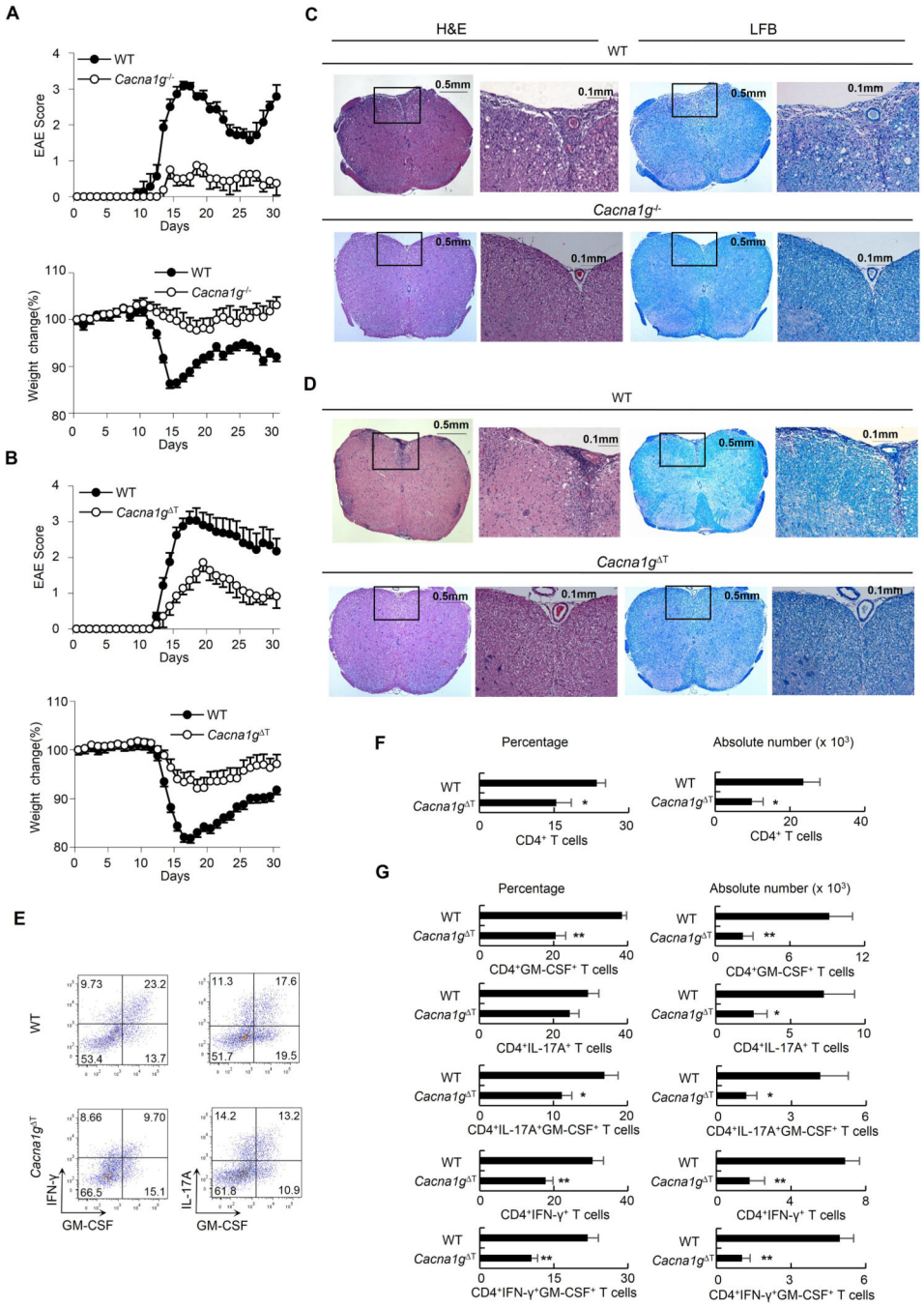

Figure 4. Resistance to EAE induction in *Cacna1g*$^{-/-}$ and *Cacna1g*$^{flox/-}$*Lck-cre* animals.

(A-B) EAE score and body weight measured daily from *Cacna1g*$^{-/-}$ mice (open circles, n = 8) and WT littermates (filled circles, n = 7) (A); and from *Cacna1g*$^{flox/-}$*Lck-cre* (open circles, n = 14) and WT littermates (filled circles, n = 16) (B) following EAE induction at day 0.

(C-D) H&E or LFB staining of spinal cord sections from WT and *Cacna1g*$^{-/-}$ mice (C) as well as WT and *Cacna1g*$^{flox/-}$*Lck-cre* EAE mice (D) at day16 EAE induction. Within each genotype the panel on the right is an enlarged view of the framed area in the left image.

(E-G) Mononuclear cells isolated from brain and spinal cord of WT and *Cacna1g*$^{flox/-}$*Lck-cre* EAE mice at day 16 after EAE induction were analyzed by flow cytometry. Representative intracellular staining for GM-CSF, IFN-γ and IL-17A in CD4$^+$ T cells (E). The percentages of CD4$^+$ T cells among mononuclear cells and absolute numbers of CD4$^+$ T cells (F) as well as percentage of GM-CSF, IFN-γ and IL-17A producing cells among CD4$^+$ T cells and absolute number of the respective population (G).

*$P < 0.05$ and **$P < 0.01$ (Mann-Whitney U test). Data are combined from two (A) and three (B) independent experiments (mean and s.e.m. in A-B). Data are from one experiment representative of three independent experiments with similar results (C-G; mean and s.e.m. in F,G). *Cacna1g*$^{\Delta T}$ refers to *Cacna1g*$^{flox/-}$*Lck-cre*. See also Figure S4.

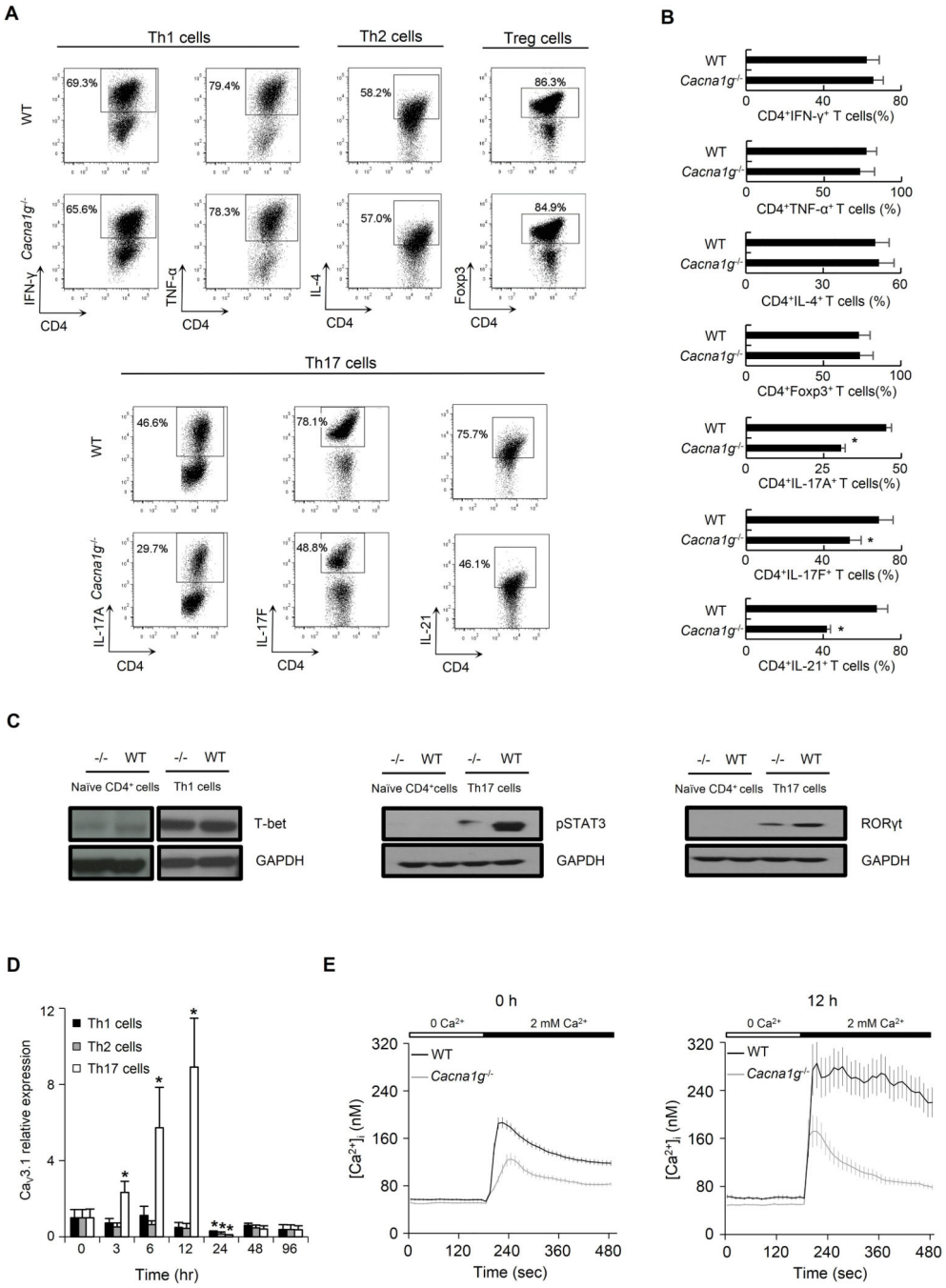

Figure 5. $Ca_V3.1$ deficiency leads to a lower percentage of Th17 cells and lower expression of Th17 transcription factors.

(A-B) Representative flow cytometry data (A) and comparison (B) of $CD4^+$ IFN-γ^+ and $CD4^+$TNF-α^+ Th1 cells, $CD4^+$ IL-4^+ Th2 cells, $CD4^+$Foxp3^+ Treg cells, and $CD4^+$IL-$17A^+$, $CD4^+$IL-$17F^+$ and $CD4^+$IL-21^+ Th17 cells following *in vitro* polarization of naïve $CD4^+$ cells from WT or *Cacna1g*$^{-/-}$ mice in Th1, Th2, Treg or Th17 culture conditions, respectively.

(C) The expressions of Th1 transcription factor, T-bet, and Th17 transcription factors, phosphorylated STAT3 and RORγt, were measured in naïve $CD4^+$ T cell and those

following *in vitro* Th1 (for T-bet) or Th17 (for pSTAT3 and RORγt) polarization from WT and *Cacna1g*$^{-/-}$ mice. GAPDH was included as loading control.
(D) Time course of $Ca_V3.1$ expression in WT naïve $CD4^+$ T cells following *in vitro* Th1 (black), Th2 (grey) or Th17 (white) polarization at 0, 3, 6, 12, 24, 48, and 96 hours. (E) Change in $[Ca^{2+}]_i$ in resting splenic naive $CD4^+$ T cells (left panel) as well as those following in vitro Th17 polarization for 12 hours (right panel) loaded with Fura-2 AM from WT (black line) or *Cacna1g*$^{-/-}$ (grey line) mice in response to 2 mM extracellular calcium. $*P < 0.05$ (Mann-Whitney *U* test). Data are from one experiment representative of three independent experiments with similar results (A-E; mean and s.e.m. in B,D,E).

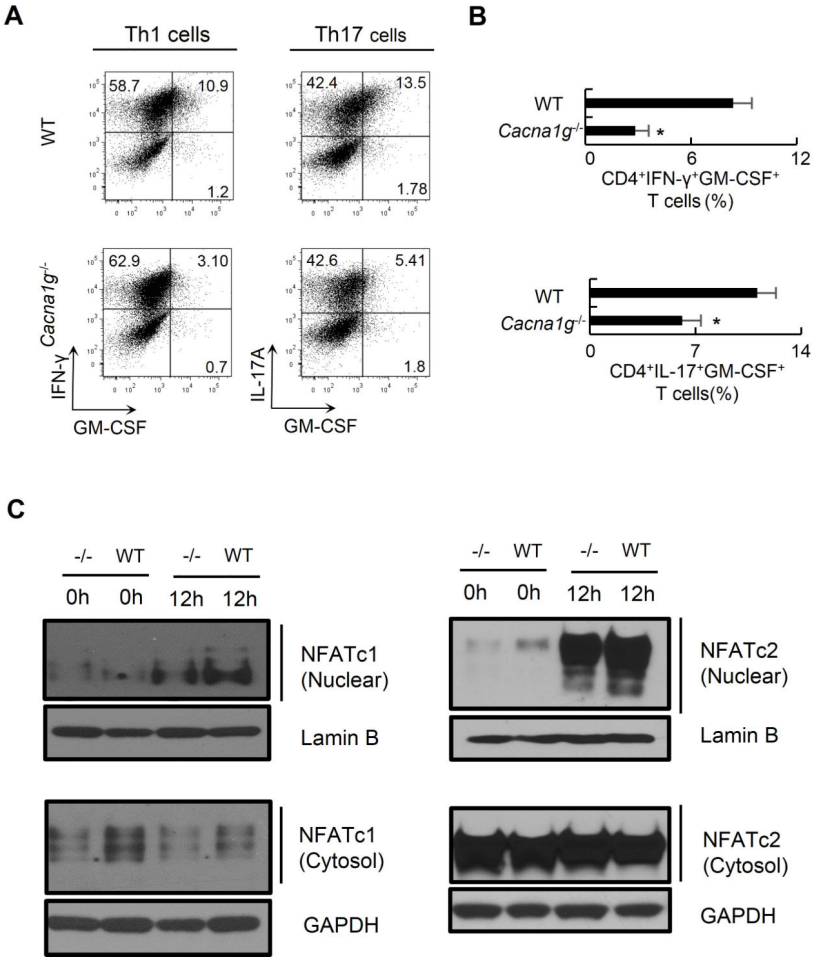

Figure 6. $Ca_V3.1$ deficiency results in reduced GM-CSF production from *in vitro* polarized Th1 and Th17 cells as well as reduced nuclear translocation of NFAT.

(A-B) Representative flow cytometry data (A) and comparison (B) of $CD4^+IFN\text{-}\gamma^+GM\text{-}CSF^+$ Th1 cells and $CD4^+IL\text{-}17A^+GM\text{-}CSF^+$ Th17 cells following *in vitro* polarization of naïve $CD4^+$ cells from WT or *Cacna1g*$^{-/-}$ mice in Th1 or Th17 cell culture conditions, respectively.

(C) Immunoblotting for NFATc1 and NFATc2 on nuclear and cytoplasmic fractions in naïve $CD4^+$ T cells and those stimulated by anti-CD3 and anti-CD28 antibodies for 12 hours from *Cacna1g*$^{-/-}$ and WT mice. Lamin B or GAPDH were included as a loading control.

*$P < 0.05$ (Mann-Whitney U test). Data are from one experiment representative of three independent experiments with similar results (A-C; mean and s.e.m. in B).

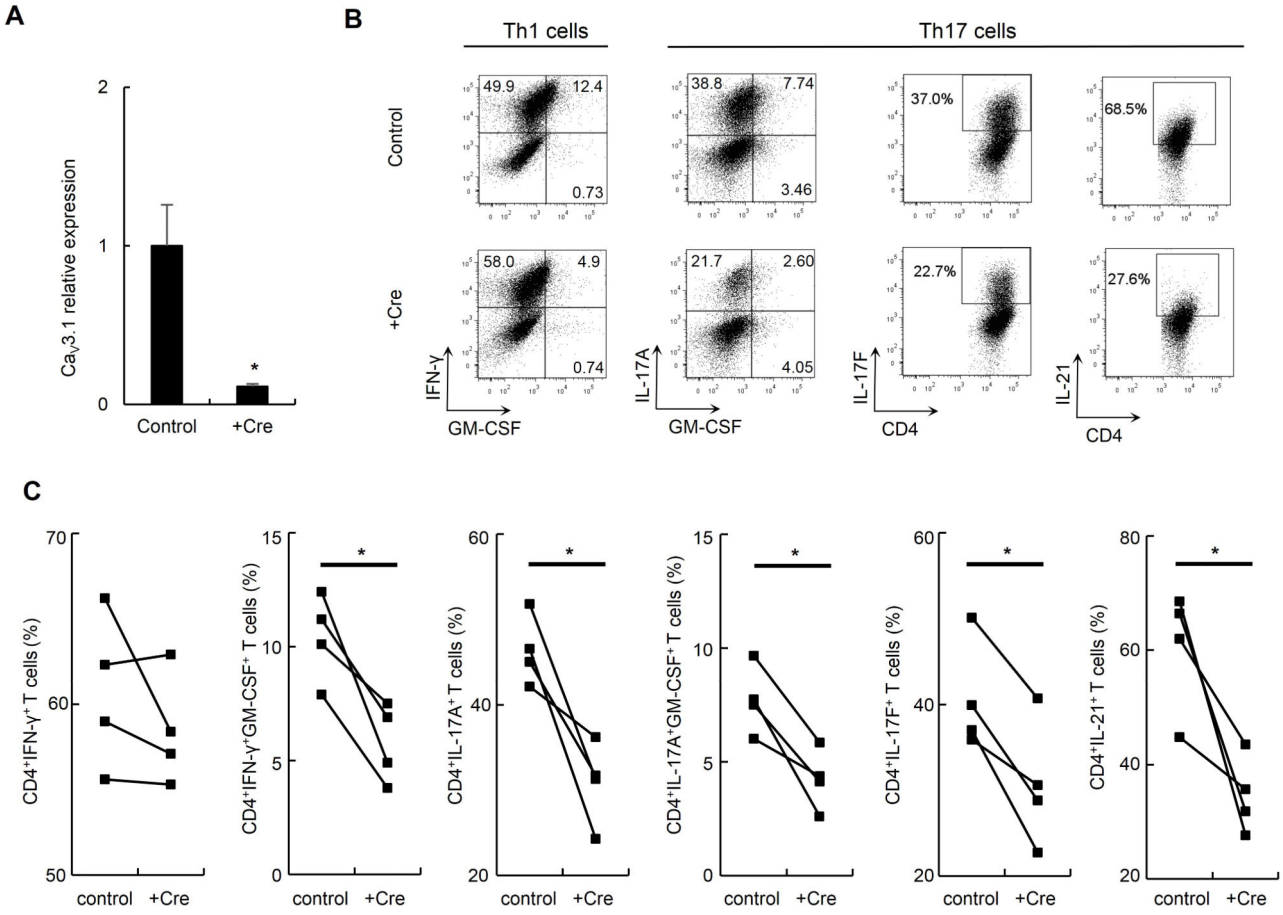

Figure 7. *Cacna1g* acute deletion alters cytokine production by *in vitro* polarized Th1 and Th17 cells.

(A) Comparison of relative expression of $Ca_V3.1$ mRNA in naïve $CD4^+$ T cells from *Cacna1g*$^{Flox/Flox}$ mice transfected with CRE recombinase lentivirus (+Cre) or empty vector (control). $*P < 0.05$ (Mann-Whitney *U* test).

(B-C) Representative flow cytometry data (B) and comparison (C) of $CD4^+$IFN-γ^+ Th1 cells, $CD4^+$IFN-γ^+GM-CSF^+ Th1 cells, $CD4^+$IL-$17A^+$ Th17 cells, $CD4^+$IL-$17A^+$GM-CSF^+ Th17, $CD4^+$IL-$17F^+$ Th17 cells, or $CD4^+$IL-21^+ Th17 cells following *in vitro* polarization of naïve $CD4^+$ cells from *Cacna1g*$^{Flox/Flox}$ mice transfected with +Cre or control virus in Th1 or Th17 cell culture conditions, respectively.

$*P < 0.05$ (paired Student *t* test). Data are from one experiment representative of three independent experiments with similar results (A-C; mean and s.e.m. in A).